Facility Location-Allocation Problem for Emergency Medical Service With Unmanned Aerial Vehicle

Youngsoo Park, Sangyoon Lee, Inkyung Sung, Peter Nielsen, and Ilkyeong Moon

***Abstract*— This paper models an operation problem of an unmanned aerial vehicle for the emergency medical service (UEMS) system. The model is set up as a location-allocation problem. The coverage distance and capacity of the UEMS facility are modeled as functions of UAVs assigned. The allocation of the demand point is constrained by the variable coverage distance of each facility. The robust optimization approach is used over the cardinality-constrained uncertain demand, which leads to a nonlinear optimization problem. The UEMS location-allocation problem (ULAP) is reformulated to a solvable problem. An extended formulation and corresponding branch-and-price (B&P) algorithm are also proposed, which strengthen the linear programming relaxation bound. The subproblem of the B&P algorithm is defined as a robust disjunctively constrained integer knapsack problem. Two solution approaches of mixed-integer linear programming reformulation and decomposed dynamic programming are designed for the subproblem. To provide time-efficient solutions for large-scale problems, a restricted master heuristic (RMH) is proposed based on the extended formulation. In computational experiments, the B&P algorithm provided a strong lower bound, and the RMH could find an effective feasible solution within an applicable computation time.**

***Index Terms*— Branch-and-price, emergency medical service, location-allocation, robust optimization, unmanned aerial vehicle.**

I. Introduction

THE medical system plays an essential role in modern society by protecting human life and health. Among the various components that constitute the medical system, the emergency medical service (EMS) system is important in connecting communities directly to the health care system. The development of and investment in the EMS system have focused on increasing the number of resources and implementing advanced equipment. However, due to the resource limitation, modern society's health care system tries to spread primary medical devices widely in public areas. One example of this is the automated external defibrillator (AED) placed in public areas. AEDs regulate the heartbeats of individuals experiencing sudden cardiac arrest and play a central role in the "chains of survival." Because rapid intervention with AEDs can secure the survival rate of patients [1], AEDs can be used to extend the "golden hour" of ambulance arrival.

In the company with the development of UAV technology, several attempts have been made to utilize UAVs in public security and health care services [2], [3], [4]. In the same manner of the commercial UAV-operated logistics [5], [6], [7], UAVs can be operated as multipurpose emergency medical resources providing rapid and flexible responses. Even though there is an increasing number of public-access AEDs in public facilities and large buildings, less than 70% and only 30% of non-residential and residential areas have an AED installed, respectively [8]. The situation worsens in suburban and rural areas, where the population is scattered over distances. Based on the limited resources, there have been attempts to cover the maximum demand by the mobile operation of AEDs [4], [8], [9]. The UAV EMS (UEMS) is also known as an "ambulance drone."

UAVs are expected to transport other medical supplies that require real-time delivery, including blood derivatives [10], [11], vaccines [12], and medications [13]. Additionally, there is an increasing amount of research that addresses the effort to transport various medical resources while focusing on the contactless characteristic of UAVs after the worst of the COVID-19 outbreak [13].

The literature on the EMS system comprises two problem environments: mass casualty and non-disaster situations. The research on mass casualty situations focuses on modeling and resolving the heavy load on the system from the instantaneous demand and the breakdown of infrastructure. Chen and Yu [14], Liu et al. [15], and Wang et al. [16] introduced temporary EMS facilities and considered EMS resource allocation. Chou et al. [17], Liu et al. [15], and Zhou et al. [18] considered evacuations and transportation of casualties under mass disaster situations. The breakdown of the transportation infrastructure was introduced in Chou et al. [17] and Liu et al. [15]. Recently, Kundu et al. [19] provided a detailed literature review of emergency logistics, which includes EMS.

The research on non-disaster situations aims to model the probabilistic demand of the public health care service and to solve the specific logistics problems, including location, relocation, and routing in a quotidian environment. Iannoni and Morabito [20], Ansari et al. [21], and

Manuscript received 8 February 2021; revised 13 December 2021 and 22 October 2022; accepted 1 November 2022. Date of publication 24 November 2022; date of current version 8 February 2023. This work was supported by the National Research Foundation of Korea (NRF) funded by the Ministry of Science, ICT & Future Planning, South Korea, under Grant NRF-2019R1A2C2084616. The Associate Editor for this article was C. G. Claudel. *(Corresponding author: Ilkyeong Moon.)*

Youngsoo Park is with Woowa Brothers Corporation, Seoul 05544, South Korea.

Sangyoon Lee is with the Samsung Advanced Institute of Technology, Samsung Electronics, Suwon-si 16678, South Korea.

Inkyung Sung and Peter Nielsen are with the Department of Materials and Production, Aalborg University, 9220 Aalborg, Denmark.

Ilkyeong Moon is with the Department of Industrial Engineering, Seoul National University, Seoul 08826, South Korea, and also with the Institute for Industrial Systems Innovation, Seoul National University, Seoul 08826, South Korea (e-mail: ikmoon@snu.ac.kr).

Digital Object Identifier 10.1109/TITS.2022.3223509

Yoon and Albert [22], [23] focused on an EMS dispatching policy-related approach based on a queuing theory. Another general approach is a location-related model. Recently, Zhang et al. [24], Park et al. [25], and Lee et al. [26] tried to tackle the EMS operation problem in a non-disaster situation through the application of a facility location problem.

Research has been related to the EMS location of the facility location models. Daskin [27] subdivided facility location models into four categories—*analytic*, *continuous*, *network*, and *discrete models*—based on the problem's space. While the continuous facility location model locates the facility in the continuous domain and can attain a true optimum, the establishment of a facility takes place on top of the current state of the region and the available sites. Furthermore, the structure of the continuous facility location problem does not include the coverage constraint in most cases, especially when there are more than two facilities to locate. One can refer to [28] and [29] for further information on the continuous facility location models. Thus, as emphasized in [27], the discrete models are dominant for health care facility locations because they focus on the discrete decisions of opening, operation, and assignments of demand points for the facilities.

There are two approaches to the discrete facility location models for the health care facility planning. The first approach is the covering-based approach. Under the given candidate locations of facilities and demand points, the feasibility of a coverage between a facility and a demand point can be considered as binary. In the covering problem, the actual distance is binarized, and the demand point is considered to be "covered" if it is in the critical coverage distance from a facility. Thus, the distance between the facility and the demand point is considered as a constraint of the problem.

The second approach is the median-based approach. In the median-based approach, the distance between the facility and the demand point is considered as a cost in the objective function, instead of a constraint. In other words, there is no limitation on the coverage distance of a facility. Any demand point can be assigned to a facility as a decision [30], [31]. One of the famous models of this concept is the location-allocation problem, which decides the facility's opening and the assignment of each demand point to that facility. The distance-weighted cost is accumulated to the objective function, in the company with the facility's opening cost. Despite of the pioneering literature considering maximum distance constraints in median-based approach as [32] and [33], the objective of the median-based approach usually focuses on the total operation cost related to the summation of the distances between every demand point and the allocated facility. The main difference between the two approaches is based on the way the distance between a facility and a demand point is considered. In the covering-based approach, the distance is binarized with the coverage distance limitation of a facility. Conversely, in the median-based approach, the demand point is allocated without any restriction, as long as the cost is valued as high enough.

However, when operating multiple UAVs in the UEMS system, the existing approaches cannot apply the characteristics of UAVs. One of the major characteristics is the physical limitation of a UAV's flight distance. Due to its payload limitation, UAVs can only cover a bounded area around the facility [4], [5], [34], [35], [36], [37]. Another characteristic is that multiple UAVs are operated in one facility within the UEMS, while only one or two ambulances are operated in one facility in the ordinary EMS system. When considering the bounded coverage distance in the existing literature, the problem is modeled with a covering-based approach. In that case, resource capacity and availability are hardly considered, so it is hard to model the effect of the number of UAVs assigned to one facility. If a location-allocation model is employed, the resource availability affected by the distribution of the demand points is considered in the cost parameter, instead of a constraint.

To locate the UEMS facility and assign multiple UAVs efficiently to facilities, the coverage distance limitation has to be considered in detail, so that the number of UAVs determines the resource availability. From the classical approaches of maximum expected covering location model [38] and maximum availability location problem [39], the *busy-fraction* of one unit of the resource was used to calculate the total resource availability by measuring the chance that at least one resource is available. With the predefined coverage area and the busy-fraction of each resource, one could calculate the expected amount of the covered demand and, on the contrary, the number of the resource required to fulfill the α*-reliability*.

We approached the busy-fraction concept from a different angle. When the number of resources increases, the coverage area can also be increased without the loss of reliability, regardless of the increased busy-fraction. In the literature on operating UAV systems, Shakhatreh et al. [40] showed that if the UAV requires a setup such as a recharge between flights, the coverage distance of the system increases along with the number of UAVs. In this research, the coverage area is modeled as the decision with the variable coverage distance. Based on the binary coverage model and covering-based approach, the variable coverage distance of a facility can be defined as the function of the resource investment [41]. The number of UAVs assigned to a UEMS facility defines the coverage distance as well as the capacity of the facility, which is introduced for the first time in this research.

The location and operation problem of the UEMS system is defined and named as a UEMS location-allocation problem (ULAP). The ULAP includes the characteristics of both covering-based and median-based approaches. The variable coverage distance constraint is modeled as a quadratic function based on the proximity of resource availability and the size of the covered area, and then reformulated into the equivalent linear formulation. Also, the allocation decision of the uncertain demand is considered with the capacity of the UEMS facility, as in the median-based approaches. A cost-minimization problem, while fulfilling every demand of the UEMS system, is modeled with a robust optimization approach. In the robust optimization approach, the demand is modeled with the cardinality-constrained uncertainty set, and the nonlinear capacity constraints are linearly reformulated. The reformulation model contains integer and continuous decision variables and has highly fractional solutions in the

linear programming (LP) relaxation. Because of the weak LP bound, the commercial optimization solvers have difficulty solving realistically-scaled problems. If the original problem is decomposed into individual facilities, each decomposed problem is related to the robust and integer knapsack problems. To utilize the knowledge of the knapsack problem, an extended formulation (EF) based on the Dantzig-Wolfe decomposition is proposed and solved by the branch-and-price (B&P) algorithm. With the B&P algorithm, the subproblem was solved by two approaches–mixed-integer linear programming (MILP) reformulation and decomposed dynamic programming (DP) approaches–each of which has its own advantages. Furthermore, a restricted master heuristic based on the B&P algorithm is proposed to provide a time-efficient feasible solution to large-sized problems.

The rest of this paper is structured as follows: Section II briefly introduces literature related to the health care facility location problem. Section III proposes the problem definition, mathematical formulation, and linear reformulation of the mathematical model. Section IV presents detailed information on the B&P algorithm of the ULAP. The extended formulation, branching strategies, structure of the subproblem, and the solution approaches of the subproblem are introduced. In addition, the restricted master heuristic for the primal solution is presented. The proposed algorithms are compared with the computational experiments in Section V. Finally, Section VI concludes the paper.

II. Related Literature

Previous literature related to the ULAP is introduced in this section. As mentioned above, there are covering-based and median-based approaches in the health care facility location problem. In the covering-based approach, to overcome the limitation of the digitized all-or-nothing coverage distance, a concept of double coverage [42] was proposed, which forced the system to cover every demand point within a large radius and, at the same time, to cover a certain proportion of the demand point within a small radius.

One limitation of the covering-based approach is the disregard of the quantity of the demand and the facility's capacity, which requires the allocation decision of the demand points to the facilities as in the location-allocation approach. In the recent works of the location-allocation approach, the demand uncertainties are investigated thoroughly with the stochastic and robust models considering the probabilities of the demand satisfaction [43]. The intractabilities of the stochastic and robust models were tackled by limiting the set of feasible facilities for each demand point or fixing policies for allocations [44]. We refer readers to the recent research of Bertsimas and Ng [45], who reviewed the probabilistic models of ambulance deployment and modeled ambulance deployment with recourse actions. In the location-allocation approach, the distance between the facility and the demand point is considered in the objective function or only filters the impossible pairs of the facility-demand point, as in [4]. Although the existing location-allocation approaches consider probabilistic constraints of the demand satisfaction, resource availability is not yet related to the decision of the size of the covered area as constraints.

TABLE I
Comparison of This Research and Existing Literature

Literature	Type	Coverage distance constraint	Demand
[42]	set cover	double coverage	binary
[39]	set cover	single coverage	binary
[33]	median	single coverage	binary
[31]	median	unconstrained	binary
[47]	set cover, median	gradual coverage	partial
[48]	median	gradual coverage	partial
[44]	median	unconstrained	uncertain
[43]	median	unconstrained	uncertain
[54]	median	unconstrained	uncertain
[45]	median	unconstrained	uncertain
[30]	median	unconstrained	binary
[4]	median	single coverage	deterministic
[49]	set cover, median	variable coverage	deterministic
[50]	median	variable coverage	deterministic
This work	set cover	variable coverage	uncertain

Two directions consider allocation decisions in the company with the covering-based approach. In the gradual cover model [45], [46], [47], [48], the demand of each demand point is "partially" satisfied by a function that decays according to the distance from a facility and modeled in the objective function. Even though the allocation is considered as decisions in the gradual cover model, the coverage distance of a facility is not modeled as constraints and cannot be treated as decisions. Another direction is the variable cover model [41], [49]. The coverage distance of a facility is treated as a decision variable, and the cost of a facility is decided by a monotonically increasing function of a coverage distance. However, the variable cover model is still bounded in the covering-based approach because the facility's capacity and the size of the demands are not considered. Thus, the demand uncertainties are hardly considered, and it is relatively simple to provide efficient feasible solutions with heuristics and metaheuristics.

To the best of the authors' knowledge, there is one existing study related to the capacity and the coverage distance [50]. However, Akl et al. [50] determined the capacity of a wireless network and used this to allocate clients to facilities, so the coverage distance and the capacity were assumed to be related inversely. Thus, the solution approaches proposed in [50] cannot be used in the ULAP. For literature focusing on health care facility location problems, we refer readers to the related review papers [51], [52], [53]. Table I compares this research to the existing literature.

III. Location-Allocation Model for UEMS Facility

A. Problem Definition

The ultimate goal of the UEMS system is to respond to medical emergencies while incurring minimum casualties. Thus, the ULAP tackles the demand uncertainty with a robust

approach. The demand uncertainty is modeled on the well-known cardinality-constrained uncertainty set [55]. To respond to perturbations in the environment, one can optimize the decision under the assumption of the maximum perturbation of every demand point with uncertainty, as proposed in [56]. Doing so can linearize the problem but has risks of making over-conservative decisions because it obligates the solution to cover every possible perturbation [57]. Thus, in the robust optimization approach, it is necessary to define the uncertainty set in a scientific manner and to optimize the decision inside of the uncertainty set. The approach is connected to the attempts to model the level of "protection." The cardinality-constrained uncertainty set used in this research was first proposed in [55] and tried to control the conservatism by restricting the total number of the demand points that might have had the maximum perturbation, instead of covering every possible realization. The research showed that one could measure the trade-off between the probability of the constraint violation and the objective value by the protection over the demand points to be realized in their maximum value. Furthermore, even when the demand realizes out of the distribution, it is well known that the solution can protect the system with a low chance of constraint violation. These observations, in some way, justify the assumption of the demand that its nominal value and the symmetric distribution are fixed and known.

In the ULAP, the number of UAVs assigned to a facility defines the capability of the facility in two ways: (1) the total capacity and (2) the coverage distance, and restricts the allocation of the demands as in Akl et al. [50]. Like ordinary capacitated facility location problems, the capacity limits the accumulated demands. Simultaneously, the capacity of a facility has to consider the individual demand point because the capacity limits the maximum distance between the facility and the allocated demand points.

While modeling the resource availability based on the variable coverage distance, we followed the concept of the variable coverage distance proposed by Berman et al. [49] and Akl et al. [50]. In this research, the variable coverage distance is modeled as a maximum coverage distance assuring a certain level of resource availability. Given the assumption that the demand is evenly distributed over the plane, the amount of covered demand increases along with the expansion of the covered area. To maintain the same resource availability, the required capacity of the facility must increase quadratically when increasing the coverage distance. These are comprised in the mathematical models in Section III-B.

The assumptions of the presented problem are defined as follows:

1) The locations of the demand point and candidate facility are already known.
2) The facility's opening cost and the purchase and operation cost per UAV of the UEMS facility are known.
3) The coverage distance of a facility is defined based on the number of the UAVs assigned to the facility.
4) The capacity of a facility is defined based on the number of UAVs assigned to the facility.
5) Every demand has to be satisfied.

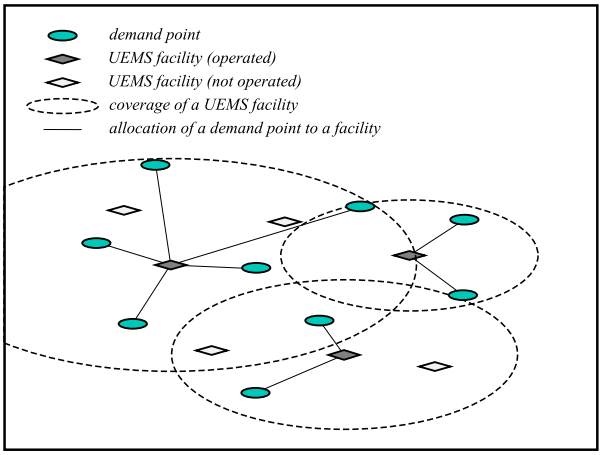

Fig. 1. Overview of the ULAP.

6) Each demand point has to be allocated to a certain facility. In other words, a partial allocation of a demand to multiple facilities is prohibited.
7) There is an upper limit to the number of UAVs assigned to a facility.
8) A demand is known with a nominal value and a value of the maximum perturbation. The uncertain demand obeys symmetric distribution, where the support is given as an interval.

Figure 1 presents an overview of the ULAP. The objective of the ULAP is to minimize the total cost to fulfill every demand while also considering uncertainties. The capacity of a UEMS facility is decided by the assignment of the UAVs, which requires the opening of the facility. The demand uncertainty is protected in the capacity constraint with a limited conservatism. That is, the ULAP considers the capacity constraint while limiting the number of the demand points with maximum perturbations. The uncertainty of the *cardinality* of the demand points is considered for each UEMS facility. Thus, the authority can control the *conservatism* of the individual facility.

B. Mathematical Formulation

The following notations are used to formulate a mathematical model of the ULAP.

Sets

I set of candidate UEMS facilities (FC).
J set of demand points (DP).

Parameters

f_i fixed cost of opening UEMS FC i.
p_i assignment cost per unit UAV at UEMS FC i.
n_i max. number of UAVs operated at UEMS FC i.
r_{0i} min. insured coverage distance of UEMS FC i.
μ_i variable coverage distance ratio per UAV of UEMS FC i.
s_{ij} distance between UEMS FC i and DP j.
$\tilde{d}_j$ uncertain demand of DP j.

Decision variables

$$y_i = \begin{cases} 1, & \text{if UEMS FC } i \text{ is opened.} \\ 0, & \text{otherwise.} \end{cases}$$

$$x_{ij} = \begin{cases} 1, & \text{if DP } j \text{ is allocated to UEMS FC } i. \\ 0, & \text{otherwise.} \end{cases}$$

$u_i \in \mathcal{Z}_+$, number of UAVs assigned at UEMS FC i.

The information of the candidate UEMS facilities is given as parameters. It includes the amortized cost related to the facility and the UAV. Also, the upper limit of the UAVs to be assigned to each facility is known. In our model, the assignment of UAVs provides a minimum insured coverage distance around a facility, and the implementation of multiple UAVs increases the coverage distance with a given variable coverage distance ratio. The ULAP models the demand uncertainty based on the cardinality constrained uncertainty set. The demand, $\tilde{d}_j$, of a demand point, j, is modeled to take value in the interval $[d_j^0 - \hat{d}_j, d_j^0 + \hat{d}_j]$ with symmetric distributions, where d_j^0 is a nominal value and $\hat{d}_j$ is a maximum perturbation. $\Gamma_i \in [0, n_i]$ is defined for each facility, i, that controls the level of conservatism. r_{0i} defines a minimum insured coverage distance over a UEMS facility opened, where the variable coverage distance is defined as an inverse quadratic function with a constant minimum value. There are three types of decision variables: two binary decision variables of the ULAP and one integer variable deciding the capacity of a facility. The standard formulation (SF) is a *compact* formulation with a nonlinear constraint.

1) Standard Formulation:

$$\min \sum_{i\in I} f_i y_i + \sum_{i\in I} p_i u_i \tag{1}$$

$$\text{s.t. } n_i y_i \geq u_i, \quad \forall i \in I \tag{2}$$

$$y_i \geq x_{ij}, \quad \forall i \in I, \forall j \in J \tag{3}$$

$$u_i \geq \sum_{j\in J} \tilde{d}_j x_{ij}, \quad \forall i \in I \tag{4}$$

$$r_{0i} + \sqrt{\mu_i u_i} \geq s_{ij} x_{ij}, \quad \forall i \in I, \ \forall j \in J \tag{5}$$

$$\sum_{i\in I} x_{ij} \geq 1, \quad \forall j \in J \tag{6}$$

$$x_{ij} \in \mathbb{B}, \quad \forall i \in I, \forall j \in J \tag{7}$$

$$y_i \in \mathbb{B}, \quad \forall i \in I \tag{8}$$

$$u_i \in \mathcal{Z}_+, \quad \forall i \in I. \tag{9}$$

Constraint (2) relates the assignment decision of UAVs to the opening of the UEMS facility and Constraint (3) links the location (opening) and allocation decisions. Constraint (6) ensure every demand to be covered. Constraint (4) bounds the allocation of the demand to the capacity of the facility. The value of the demand is calculated as the number of UAVs required. The uncertainty of the demand is not described in the controllable format yet. In the cardinality constrained uncertainty set, we optimize the objective function against every scenario in which the uncertain demand is realized, as long as the number of demand points with extreme perturbation is lower than the target protection level Γ_i. According to [55], Constraint (4) can be modeled for each facility, i, as:

$$u_i \geq \sum_{j\in J} \tilde{d}_j x_{ij} = \sum_{j\in J} d_j^0 x_{ij} + \max_{N\subseteq J, |N|=\Gamma_i} \sum_{j\in N} \hat{d}_j x_{ij} \tag{10'}$$

Note that Constraint (4) is still nonlinear. Constraint (5) is a quadratic constraint that defines the variable coverage distance around a facility. The coverage distance is defined as a summation of a minimum insured coverage distance and the variable distance related to the number of UAVs and the variable coverage ratio. Although we modeled the variable coverage as a quadratic constraint because of its simplicity, other monotonic non-decreasing (e.g., linear or piecewise-linear) functions can be utilized instead of the quadratic function. One can refer to the literature related to resource availability and the busy-fraction [39], [48], [58], [59].

C. Linearization of the Quadratic Variable Coverage Distance Function

Let a parameter CV_{ij} denote the coefficient of coverage distance between facility i and demand point j:

$$CV_{ij} := \begin{cases} 0, & \text{if } r_0 \geq s_{ij}. \\ \dfrac{(s_{ij} - r_{0i})^2}{\mu_i}, & \text{otherwise.} \end{cases}$$

Considering Constraints (7) and (9), an equivalent linear reformulation of Constraint (5) is proposed:

Proposition 1: The following inequality $u_i \geq CV_{ij} x_{ij}$ is equivalent to Constraint (5) *for the ULAP.*

Proof: We only have to consider facility i and demand point j which satisfies $s_{ij} \geq r_{0i}$.

($\Rightarrow$) Let $\mu_i u_i \geq (s_{ij} - r_{0i})^2 x_{ij}$ for facility i and demand point j. (i) $x_{ij} = 1$, $\mu_i u_i \geq (s_{ij} - r_{0i})^2 \Longrightarrow \mu_i u_i \geq (s_{ij} x_{ij} - r_{0i})^2$. (ii) $x_{ij} = 0$, $\mu_i u_i \geq 0 \Longrightarrow r_{0i} + \sqrt{\mu_i u_i} \geq 0$.

($\Leftarrow$) Let $\mu_i u_i \geq (s_{ij} x_{ij} - r_{0i})^2$. $(s_{ij} x_{ij} - r_{0i})^2 \geq x_{ij}(s_{ij}^2 x_{ij} + r_{0i}^2 - 2 s_{ij} x_{ij} r_{0i})$ ($\because x_{ij} \leq 1$). In both cases of $x_{ij} \in \mathbb{B}$, $\mu_i u_i \geq (s_{ij} - r_{0i})^2 x_{ij}$ holds. □

Based on Proposition 1, Constraint (5) can substitute for Constraint (5):

$$u_i \geq CV_{ij} x_{ij}, \quad \forall i \in I, \ \forall j \in J. \tag{11'}$$

D. Linear Reformulation of Standard Formulation

The standard formulation with nonlinear constraint can be reformulated into an equivalent linear formulation using the dual of the inner optimization problem [55]. The reformulation is provided as follows:

1) Reformulated Standard Formulation:

$$\min \ (1)$$

$$\text{s.t. } (2), (3), (5), (6), (7) - (9)$$

$$u_i \geq \sum_{j\in J} d_j^0 x_{ij} + \alpha_i \Gamma_i + \sum_{j\in J} \beta_{ij}, \quad \forall i \in I \tag{12}$$

$$\alpha_i + \beta_{ij} \geq \hat{d}_j x_{ij}, \quad \forall i \in I, \ \forall j \in J \tag{13}$$

$$\alpha_i \geq 0, \quad \forall i \in I \tag{14}$$

$$\beta_{ij} \geq 0, \quad \forall i \in I, \ \forall j \in J. \tag{15}$$

The decision variable β_{ij} is an auxiliary variable used for the linearization of the inner optimization problem of Constraint (4). α_i is the dual variable of the linearized inner optimization problem. Constraint (12) defines the capacity constraint of a facility, which uses a protection function to linearize Constraint (4). Constraint (13) is the dual of the linearized inner optimization problem. For detailed information on the reformulation procedure, one can refer to [55]. Note that the reformulated standard formulation (RSF) consists of linear constraints with binary, integer, and continuous decision variables. The problems in the RSF can be solved with commercial optimization solvers (e.g., Cplex, Xpress, and Gurobi). However, the commercial solvers that utilize LP relaxation-based branch-and-cut algorithms have difficulty solving the large-sized problems in the RSF within a short computation time, even though the solvers can handle relatively large-sized nominal problems within reasonable computation times. This is because the combination of the integer and continuous decision variable generally causes the highly fractional solution of the LP relaxation and have a weak LP relaxation bound [60].

IV. Solution Algorithms

A. An Extended Formulation of the ULAP

The solution of the ULAP consists of individual decisions about each facility, which constructs a set-partitioning structure. Based on the Dantzig-Wolfe decomposition, one can reformulate the decisions of the SF with *column-wise* decisions. Each column in the extended formulation defines a set of demand points covered by a facility and the minimum number of UAVs required for the allocation. In other words, based on each facility, several feasible allocation of the set of demand points are given in advance, along with the required number of UAVs. Ω_i is a set of feasible columns for a facility, i. A column is defined as a combination of the subset of the demand points that can be allocated to a facility and the number of UAVs required to cover the demand points. The parameters and the decision variables of the extended formulation are presented as follows:

Parameters

c_{ik} cost associated to column k of FC i.
w_{ij}^k indicate whether FC i covers DP j in column k.
u_i^k number of UAVs assigned to FC i in column k.

Decision variables

$$z_{ik} = \begin{cases} 1, & \text{if column } k \text{ is used by FC } i. \quad \forall i \in I, \\ 0, & \text{otherwise.} \qquad\qquad\quad \forall k \in \Omega_i \end{cases}$$

The cost of each column is defined as $c_{ik} := f_i + p_i u_i^k$. The extended formulation (EF) model of UEMS is represented in the following integer program:

1) Extended Formulation:

$$\min \sum_{i \in I} \sum_{k \in \Omega_i} c_{ik} z_{ik} \tag{16}$$

$$\text{s.t.} \sum_{i \in I} \sum_{k \in \Omega_i} w_{ij}^k z_{ik} \geq 1 \quad \forall j \in J \tag{17}$$

$$\sum_{k \in \Omega_i} z_{ik} \geq 1 \quad \forall i \in I \tag{18}$$

$$z_{ik} \in \mathbb{B} \quad \forall i \in I, \ \forall k \in \Omega_i \tag{19}$$

The extended formulation only remains the set-partitioning structure, while the capacity-related and coverage-distance-related constraints are considered implicitly in the column. Let us call the LP relaxation of the extended formulation the *master problem*. The LP dual of the master problem can be viewed as the Lagrangian dual, which is better than the LP bound of the standard formulation. By Minkowski's theorem, every solution of the compact formulation can be represented in the extended formulation. If Ω_i contains every feasible column for every facility i, then the solution set of the master problem defines the convex hull of the ULAP. However, this requires an exponential number of columns. To avoid maintaining a very large number of variables, the column generation (CG) technique can be implemented to solve the Lagrangian dual. The CG iterates between the restricted master linear problem (RMLP) and the pricing subproblem while generating new variables that might improve the current solution. Let π_j and σ_i be dual prices associated with Constraints (17) and (18). The pricing subproblem can be defined for each facility i:

2) Pricing Subproblem:

$$\min \ f_i + p_i u - \sum_{j \in J} \pi_j x_j + \sigma_i \tag{20}$$

$$\text{s.t. } u \geq \sum_{j \in J} d_j^0 x_j + \max_{N \subseteq J, |N| = \Gamma_i} \sum_{j \in N} \hat{d}_j x_j, \tag{21}$$

$$u \geq C V_{ij} x_j, \quad \forall j \in J \tag{22}$$

$$u \leq n_0 \tag{23}$$

$$x_j \in \mathbb{B}, \quad \forall j \in J \tag{24}$$

$$u \in \mathcal{Z}_+. \tag{25}$$

The pricing subproblem of ULAP can be defined as a *robust integer knapsack problem*. The robust integer knapsack problem includes integer decision variables in the capacity constraint [61], [62]. The integer decision variable acts as a supplementary capacity that can be purchased additionally from the original capacity. Constraint (21) is nonlinear and can be reformulated as in the RSF. If Constraint (21) is reformulated with the robust counterpart, the pricing subproblem gets a characteristic of a robust mixed-integer linear knapsack problem because of the integer decision variable u_i and the continuous variables α_i and β_{ij}. Constraint (22) hunts down the demand points that cannot be covered by the given coverage distance, and zeroes out the decision variable, x_j, of the demand points. On the other hand, when the number of UAVs assigned to a facility is fixed, it becomes a robust 0-1 knapsack problem. Therefore, the pricing subproblem can be solved by a decomposed approach that solves multiple 0-1 robust knapsack problems. The number of the decomposed 0-1 robust knapsack problems equals to n_i, the maximum number of UAVs to be operated at the UEMS facility i.

B. Branching Strategy

The column generation iterates between the restricted master problem and the pricing subproblem. The solution of the

master problem can be translated into the solution space of the original (standard formulation) variable. However, because the master problem is the LP relaxation of the extended formulation, the translated solution is not necessarily an integer when the column generation process is solved to the optimal. The branch-and-price algorithm applies the CG to solve each node in the branch-and-bound procedure, and can execute branching when the solution of the CG is fractional.

The branching in the B&P algorithm can be executed with various strategies [63]. First, the branching can be executed over the variables of the extended problem. However, it is generally difficult to formulate the branching decision explicitly in the variables of the pricing problem, and can complicate the solution algorithm. Also, binary fixing of one among many columns provides an unbalanced branch-and-bound tree, which weakens the effect of the branching.

In the second strategy, branching over the original variables of the standard formulation can be used. In the ULAP, for a facility i, if the decision variable x_{ij} is decided for every demand point j, then the minimum value of u_i can be calculated subsequently:

$$u_i = \max\left\{\lceil\sum_{j\in J} x_{ij}d_j\rceil, \lceil[(x_{ij}s_{ij} - r_i^0)^+]^2/\mu\rceil\right\}.$$

Thus, the branching can be defined based on the decision variable x_{ij}. When the CG provides a fractional solution of the original variable x_{ij}, the branching creates two children nodes separated by the allocation between a demand point and a facility. The second strategy shows a more balanced branch-and-bound tree, so it is commonly used for various applications (e.g., generalized assignment problems). One strength of the branching on original variables is that the branching decision does not complicate the pricing subproblem. In the robust knapsack problem, fixing the allocation of a demand point can be applied by adjusting the remaining capacity of the facility. Thus, the branching only changes the parameters of the pricing subproblem while maintaining the structure of the problem. However, in the ULAP, binary fixing of one decision variable x_{ij} still provides an unbalanced branching and has a small impact, where we observed the inefficiency.

The third strategy is the Ryan-Foster [64] branching rule. When the master problem has a set-partitioning-like characteristic over a pure binary subproblem, the branching decision can be made based on the coexistence of two elements. We applied the Ryan-Foster branching rule, which showed the best performance based on the model of the balanced branching tree. However, because the ULAP does not originally include conflict constraints, unlike edge coloring and bin packing with conflict [65], the implementation of the Ryan-Foster branching rule changes the structure of the pricing subproblem. Therefore, we redefined the pricing subproblem, especially in order to implement the special-purpose solver for the subproblem. In the Ryan-Foster branching rule, the fractional solution of the restricted master problem denotes the (fractional) employment of a feasible column. Based on the fractional solution of the CG, the degree of the coexistence of a pair of demand points, v_{j_1,j_2}, can be measured. If a column, $k \in \Omega_i$, includes both demand points j_1 and j_2, then the optimal solution of the column, z_{ik}^*, can be added to measure the degree of the coexistence of the pair of demand points j_1 and j_2. One can calculate it for every pair of demand points in the same way: $v_{j_1,j_2} := \sum_{k\in\Omega_i, w_{i,j_1}^k = w_{i,j_2}^k = 1} z_{ik}^*$. When the degree of coexistence is nearest to 0.5, then the pair of demand points is chosen for the branching.

C. Robust Disjunctively Constrained Integer Knapsack Problem

As mentioned in Section IV, the pricing subproblem of the ULAP is related to the robust integer knapsack problem. The Ryan-Foster branching provides two children, one forcing and the other forbidding the coexistence of two demand points. The former is called *same-child*, and is easy to be considered in the special-purpose solver by introducing an auxiliary demand point merging two demand points. However, the latter *differ-child* destroys the special structure of the knapsack problem. The conflict, or disjunctive constraint, in the knapsack problem is notorious for its simple shape and difficulty. The disjunctively constrained knapsack problem (DCKP) was defined by Yamada et al. [66] and drew more attention because of its equivalence [65], [67] to the pricing subproblem of the bin packing problem with conflict (BPPC).

In Section IV-E, the generic branching scheme [68] is used to implement the Ryan-Foster branching in the ULAP and consider the following arbitrary conflict. Based on the conflict relation between demand points defined by the branching, we defined the feasible set and solved the pricing subproblem individually. As a matter of convenience, we call the subproblem of the ULAP a robust disjunctively constrained integer knapsack problem (RDCIKP). In this paper, two solution approaches are proposed to solve the RDCIKP. In Section IV-D, we find linear reformulation of the RDCIKP and solve with the MILP solver. In Section IV-E, the RDCIKP is decomposed into multiple 0-1 knapsack problems and solved with the dynamic programming algorithm. In the computational experiment, we used a hybrid algorithm using both approaches alternately.

D. MILP Reformulation Approach

By using the techniques of Bertsimas and Sim [55], the linear reformulation of the RDCIKP for a facility i is derived:

1) Linear Reformulation of the RDCIKP:

$$\begin{aligned}
&\min\ (20)\\
&\text{s.t. } (22)-(25)\\
&\quad u \geq \sum_{j\in J} d_j^0 x_j + \alpha\Gamma_i + \sum_{j\in J}\beta_j, && (26)\\
&\quad \alpha + \beta_j \geq \hat{d}_j x_j, \quad \forall j \in J && (27)\\
&\quad \alpha \geq 0, && (28)\\
&\quad \beta_j \geq 0, \quad \forall j \in J. && (29)
\end{aligned}$$

When branching happens in a node of the branching tree, if the demand points j_1 and j_2 are chosen, then an additional constraint, $x_{j_1} = x_{j_2}$, is added to every subproblem of the same-child node, regardless of the facility. On the other hand,

a more complicated constraint, $x_{j_1} + x_{j_2} \leq 1$, is added to every subproblem of the differ-child node. As in the reformulated standard formulation, the nonlinear capacity constraint is linearized using the dual variable of the inner optimization problem. The formulation consists of the binary, integer, and continuous decision variables, which give rise to the weak LP bound. In the early stages of the CG process, linear reformulation of the RDCIKP can be solved within a short computation time with a commercial solver. However, as the CG progresses and the dual bound converges to the optimal dual solution of the master problem, it gets difficult and takes time to solve the pricing subproblem. Thus, a decomposed DP approach is designed to use a special-purpose solver to solve the RDCIKP, as presented in the next section.

E. Decomposed DP Approach

The 0-1 knapsack problem is one of the most studied problems and is well known to be solved by dynamic programming in pseudo-polynomial time. To take advantage of the knapsack problem, we propose a decomposed-based approach in this research. From the ideas of Bertsimas and Sim [69], the RDCIKP is decomposed into nominal 0-1 knapsack problems, based on the combination of the feasible sets.

Bertsimas and Sim [69] showed that the robust 0-1 knapsack problem could be solved by solving $|J| + 1$ nominal 0-1 knapsack problems. Lee et al. [70] reduced the number of nominal problems into $|J| - \Gamma + 1$. On the other hand, as shown in Section IV-C, if the number of UAVs assigned to a facility is fixed, then the RDCIKP becomes a robust disjunctively constrained 0-1 knapsack problem. Thus, the RDCIKP can be decomposed by the number of UAVs, u. For the disjunctive constraint, Pferschy and Schauer [71] proposed a pseudo-polynomial algorithm for the DCKP with chordal conflict graphs. However, the ULAP consists of the arbitrary conflict relation, which requires the enumeration of the feasible set. Let us consider the feasible set of a RDCIKP of facility i defined as:

$$\begin{aligned} S &= \Big\{x \in \mathbb{B}^m, u \in \mathcal{Z}_+ \Big| u \geq \sum_{j\in J} d_j^0 x_j + \max_{M\subseteq J, |M|=\Gamma_i} \sum_{j\in N} \hat{d}_j x_j, \\ &\quad u \leq n_0, u \geq CV_{ij}x_j, \quad \forall j \in J, x \in \mathcal{B}\Big\} \\ &= \Big\{x \in \mathbb{B}^m, u \in \mathcal{Z}_+ \Big| u \geq \sum_{j\in J} d_j^0 x_j + \sum_{j\in J'} \hat{d}_j x_j, u \geq CV_{ij}x_j, \\ &\quad u \leq n_0, \quad \forall j \in J, \ \forall J' \subseteq J \text{ with } |J'| = \Gamma_i, x \in \mathcal{B}\Big\} \end{aligned}$$

where $\mathcal{B}$ is the family of all the subsets of demand points that are not in conflict. In practical implementation, we developed independent sets of the given conflict graph with enumeration. The demand points, without any disjunctive constraint, were then added to each independent set, which formed a feasible set, $\mathcal{B}$.

Following the notations of Lee et al. [70], let us define sets $L = \{\Gamma_i, \Gamma_i + 1, \ldots, m-1, m+1\}$ and $S_{ul} = \{x \in \mathbb{B}^m | u - \Gamma_i \hat{d}_l \geq \sum_{j\in J} d_j^0 x_j + \sum_{j\in J_l} (\hat{d}_j - \hat{d}_l) x_j, u \geq CV_{ij}x_j, \forall j \in J\}$, where $J^+ = J \cup \{m+1\}$, $l \in J^+$, and $J_l = \{j \in J^+ | j \leq l\}$. By the following proposition, the RDCIKP can be solved by solving at most $2^E n_i(|J| - \Gamma_i + 1)$ nominal 0-1 knapsack problems, where E is the number of the disjunctive constraints of the RDCIKP.

Proposition 2: The RDCIKP

$$Z^* = \max\Big\{\sum_{j\in J} \pi_j x_j - f_i - \sigma_i - p_i u \Big| (x,u) \in S, x \in \mathcal{B}\Big\}$$

can be solved by solving at most $n_i(m - \Gamma_i + 1)$ *nominal disjunctively constrained 0-1 knapsack problems*

$$Z_{ul}^* = \max\Big\{\sum_{j\in J} \pi_j x_j - p_i u \Big| (x,u) \in S_{ul}, x \in \mathcal{B}\Big\}, \quad \forall u \in \{0,\ldots,n_i\}, l \in L$$

Proof: Note that f_i and σ_i are given parameters. For every $u \in \{0,\ldots,n_0\}$, let us define a set $S_u = \{x \in \mathbb{B}^m | u \geq \sum_{j\in J} d_j^0 x_j + \max_{M\subseteq J, |M|=\Gamma_i} \sum_{j\in N} \hat{d}_j x_j, u \geq CV_{ij}x_j, \forall j \in J\}$ which is a subset of S. Because $S = \bigcup_{u=0}^{n_i} S_u$, Z^* can be solved by solving at most n_i robust disjunctively constrained 0-1 knapsack problems. By Lee et al. [70], each robust disjunctively constrained 0-1 knapsack problems can be solved by solving at most $|J| - \Gamma_i + 1$ nominal disjunctively constrained 0-1 knapsack problem. □

The feasible set, $\mathcal{B}$, used in the proposition is defined based on the independent set, which has cardinality at most 2^E. By the rule of product of the nested loop, the RDCIKP can be solved in $O(2^E n_i^2 |J|^2)$.

F. Hybrid Algorithm of the Solution Approach

In Section IV-C, it is shown that the subproblem of the CG process is the RDCIKP. Because the computation speed of the overall CG algorithm heavily depends on the efficiency of solving its subproblem, it is natural to utilize both approaches developed through the previous sections. In the initial stage of the CG process, it is easier to solve the RDCIKP with the MILP reformulation approach because of a large gap between the optimal solution of the RMLP and the Lagrangian dual bound. The decomposed DP approach takes advantage of the special-purpose solver of the knapsack problem. The decomposed DP approach can provide the solution in a robust manner because the computation time is consistent, regardless of the progress of the CG and the corresponding convergence of the bound.

To benefit from both approaches, a hybrid algorithm was used in this research. In the early stage of the CG process, the MILP reformulation approach was used to solve the pricing subproblem. When the subproblem is solved by the MILP reformulation approach, there was a tendency of the computation time of each iteration to increase in accordance with the CG process. Thus, after each iteration of the CG algorithm, the time was measured. If the time of an iteration exceeded a predefined criterion, the solution algorithm of the subproblem was switched into the decomposed DP approach, which maintains a certain computation time regardless of the CG stages. The limitation of the time for the change of the solver was chosen arbitrarily to be 100 seconds in the experiment.

G. Restricted Master Heuristic

Despite the better LP bound of the CG, the B&P algorithm can take a long enumeration of branching on the large-sized problem, resulting in a long computation time. To solve the large-sized problem in a feasible computation time, we implemented the *restricted master heuristic (RMH)*, one of the most widely used heuristics related to the B&P algorithm. Based on the current variables (columns), one can solve the ULAP with the extended formulation using MILP solvers. This is also called *price-and-branch*, because the columns are generated first, and the branching takes place later. It is not guaranteed that all the values required are found before starting to solve the master integer problem, so the solution of the heuristic can only be used as a primal bound of the ULAP. Note that the RMH can be initiated in any stage of the B&P algorithm, especially before the termination of the root node CG.

Although there are advanced heuristics, including the diving heuristic [72], developed for the B&P algorithm, they are challenging to implement in the ULAP. Note that the best-first search strategy is implemented in the B&P algorithm to maximize the advantage of the Lagrangian dual bound. The diving heuristics are developed based on the depth-first search, which complicates the utilization of the heuristics in the ULAP. One alternative is the relax-and-fix algorithm on the original variables. It also has difficulty with the highly fractional solution of the LP relaxation induced by the robust counterpart and the following continuous decision variables. As mentioned in Section IV-B, fixing one decision variable, x_{ij}, did not provide a dramatic effect on the residual problem. Also, there is a feasibility issue using the relax-and-fix algorithm in the ULAP because of the capacity constraint.

The RMH can be implemented inside of the B&P algorithm to provide the primal bound. Furthermore, if there is a substantial restriction on the computation time, the heuristic can be used to provide a feasible solution, which is presented in Section V.

V. Computational Experiments

Computational experiments were conducted to compare the performance of the proposed solution algorithms. The models were developed in FICO Xpress 8.5 and solved with Xpress-Optimizer 33.01.02. Experiments were performed with an AMD Ryzen ™ 7 2700X 8-Core CPU at 3.70GHz and 32GB of RAM running on a Windows 10 64-bit operating system.

A. Datasets Used in the Experiments

Small and large-sized datasets were randomly generated for computational experiments, using the simple plant location problem on a Euclidean plane, with benchmark data from the Benchmark Library [73]. Three small-sized and two large-sized problem classes were tested, and 10 instances are generated for each problem class. The demand points were distributed randomly on the interior of a given size of a square on the Euclidean plane. Figure 2a and Figure 2b show solutions of a small and large-sized problem, respectively.

For each problem class, the maximum number of UAVs operated at the UEMS facility, the minimum ensured coverage distance, and the variable coverage distance ratio per UAV were determined for the realistic UEMS system in regard to both capacity and coverage distance, both of which can affect the number of UAVs assigned to a facility. The parameters related to the number of UAVs, capacities, and coverage distances are presented in Table II. In the table, NI and NJ represent the number of candidate facilities and the demand points, respectively. $Slim$ refers to the size of the plane.

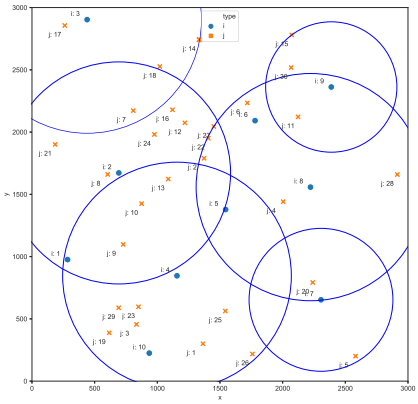

(a) RSF solution of C130.

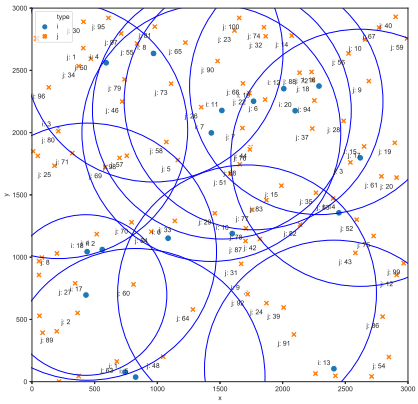

(b) RMH solution of C2100.

Fig. 2. Example of the solution.

The demand for each demand point was randomly generated based on uniform distribution. The nominal value of the demand d_j^0 and its maximum perturbation $\hat{d}_j$ are generated following U[0, 3] and U[0, $d_j^0/1.3$], respectively. The opening cost and operation (assignment) cost per unit UAV were generated based on Shavarani et al. [74], which followed U[300,000, 400,000] and U[30,000, 40,000], respectively. One can refer the dataset instance used in this research [75].

B. Algorithmic Performances

First, we compared the algorithmic performances of the two formulations, the RSF and the EF. The tightness of the LP relaxation bounds and the induced lower bounds were compared, along with the optimality of the primal bounds. Second, a further analysis of the B&P algorithm was conducted. Third, the performances of the restricted master heuristics were analyzed.

TABLE II
PARAMETERS OF THE PROBLEM CLASSES

Problem Class	NI	NJ	Γ	n_i	r_{0i}	μ_i	$Slim$
C11	10	10	3	20	500	200,000	5,000
C13	10	30	4	15	300	25,000	3,000
C23	20	30	4	12	300	25,000	3,000
C210	20	100	10	20	400	20,000	3,000
C320	30	200	10	20	500	200,000	5,000

For the first analysis, the computation speed was compared based on the computation time and the final gap between the best value of the feasible solution (BFS) and the best lower bound (BB). The optimality of the BFS was also compared, and the strength of the formulation was shown based on the tightness of the LP relaxation and the final BB. In the computation, the maximum time limit was set to 3,600 seconds. In Tables III – V, the results are summarized by the average of 10 instances of each problem class. The columns in these tables are defined as follows:

- $\#solved$: the number of the instances in the problem class, solved by each algorithm.
- $Time$: the average of the computation time. For the problems not solved within the computation time limit, the limit was used as the computation time while calculating the average, and was marked with an asterisk (*).
- $GapL$: the average of the gap between the primal bound (the best feasible solution: BFS) and the best lower bound (BB). $GapL$ is used to evaluate the algorithm's convergence speed, especially for the problems not solved to optimal within the time limit. $Gap_L = \frac{(\text{BFS})-(\text{BB})}{(\text{BFS})} \times 100\%$
- Rat_{LP}: the average of the ratio between the LP relaxation bounds of the reformulated standard formulation and the extended formulation. $Rat_{LP} = \frac{(\text{LP bound of the EF})}{(\text{LP bound of the RSF})} \times 100\%$

The pricing subproblem is identical to the Lagrangian relaxation subproblem, and can be used as a lower bound of the RMLP [76]. Thus, in the CG of the root node, the dual bound of a pricing subproblem can be used as a lower bound of the problem, regardless of the termination of the CG. On the other hand, in the B&P algorithm, we implemented the best-first search (BS) for the search strategy. Because the lower bound of the head node of the active node queue always has the *worst* lower bound in the BS, it can be used as a lower bound of the problem. For the problems that the B&P algorithm has not finished within the time limit, the lower bound calculated by the BS was used for the comparison in Table IV. In the same table, if the root node CG was not finished, the lower bound of the RMLP was used as the LP relaxation bound and marked with an asterisk (*).

The average of the overall instances of each problem class is calculated in Table III. In the small-sized problems, the commercial solver's root cutting and heuristic techniques showed powerful performances while solving the RSF. Even the integer feasible solutions provided by the root cutting and heuristics were optimal solutions in several small-sized problems. The B&P algorithm could solve the problem within a short computation time without both a heuristic and a valid inequality, due to the advantage of the LP relaxation bound. In the large-sized problems, the root node CG of the problem class C210 was solved within the time limitation, but the overall B&P was not finished as well as the RSF. If an algorithm failed to solve every instance in a problem class, the average computation time was marked to be the time limit 3,600. The size of the problem class C320 was too big to be solved by any algorithm. However, the progress of the optimization, including the CG and the RMH algorithm, was compared later.

$GapL$ compares the convergence between the BFS and the BB of algorithms. In the problem classes C210 and C320 of the B&P algorithm, the BFS was not provided, so it was impossible to calculate the $GapL$. As mentioned above, the commercial solver could provide effective feasible solutions of the RSF with root cutting and heuristics. When implemented in real-world cases, those techniques could be utilized in the B&P algorithm by providing the feasible columns and the primal bounds. In this computational experiment, we investigated the advantages of the EF in the BB perspective. Thus, the LP bound and the lower bound provided by the following branching are compared in Table IV, without consideration of additional techniques, such as valid inequalities and heuristics.

As mentioned in Section IV-A, the LP bound of the EF was always the same or better than the LP bound of the RSF. Indeed, as illustrated in Table IV, the LP relaxation bound of the EF was better than the RSF from 1.7% to 81.1%, and the overall average of the Rat_{LP} was 138.8%. In the problem class C320, the LP bound has the same value of the BB because the root node column generation was not solved to the optimal. It was expected that the gap of the LP bound between the RSF and the EF would increase when the CG was finished. As the optimization process continued, the Gap of the BB was marked as zero if both algorithms found the optimal solution. There was a minus gap of the lower bound in the problem class C23, which took place because of the two unfinished instances of the B&P algorithm. As the size of the problem increased, the gap of the lower bound between the RSF and the B&P algorithms deepened.

In the optimality perspective of the small-sized problems, in Table V, there is no gap between the two algorithms because both algorithms found the optimal solution for every problem. In the large-sized problems, the B&P algorithm could not find feasible integer solutions. In this research, the B&P algorithm employed the best-first search to utilize the advantage of the lower bound. The depth of the branching tree does not deepen fast in the BS, so it is difficult to find the primal solution. Although the primal heuristic, such as the RMH, can help to find the feasible solution, it was not used in this experiment to examine the primary performance of the EF and the B&P themselves. The performance of the RMH will be investigated in the latter part of this paper.

For the second analysis, the nodes and the columns generated in the B&P algorithm are summarized in Table VI. The effectiveness of the EF and the column generation algorithm are analyzed in Table VII. The columns in the tables are defined as follows:

TABLE III
RESULTS RELATED TO THE COMPUTATION SPEED

Problem Class	# solved			Time (s)			GapL (%)	
	RSF	CG	B&P	RSF	CG	B&P	RSF	B&P
C11	10	10	10	0.06	0.05	0.44	0.0	0.0
C13	10	10	10	0.25	0.47	8.52	0.0	0.0
C23	10	10	8	1.15	0.79	974.36*	0.0	0.6
C210	0	10	0	3,600*	1,294.63	3,600*	7.1	-
C320	0	0	0	3,600*	3,600*	3,600*	34.3	-

$*$: There are instances not solved within the time limit.
$-$: There is no instance that provided a BFS within the time limit.

TABLE IV
COMPARISON OF LP RELAXATION

Problem Class	LP relaxation bounds			Lower bounds		
	RSF	EF (CG)	Rat_{LP} (%)	RSF	B&P	Gap (%)
C11	770,575	993,507	127.7	1,029,704	1,029,704	0.0
C13	1,878,139	3,082,336	164.4	3,125,399	3,125,399	0.0
C23	2,108,738	3,069,304	146.4	3,202,811	3,184,722	-0.6
C210	4,968,062	6,269,128	126.1	6,037,631	6,269,589	3.8
C320	9,252,454	11,975,240*	129.4	9,894,785	11,975,240*	21.0

$*$: There are instances with the unfinished root node CG.

TABLE V
RESULTS RELATED TO THE OPTIMALITY

Problem Class	RSF	B&P	
	BFS	BFS	Gap (%)
C11	1,029,705	1,029,704	0.0
C13	3,125,400	3,125,399	0.0
C23	3,202,813	3,202,813	0.0
C210	6,507,051	-	-
C320	15,484,665	-	-

$-$: No BFS is found within the time limit.

- *Cols* and *Nodes*: the average number of columns and nodes generated in the CG and the B&P algorithms. If a problem class contains instances not solved within the computation time limit, the number of the columns or nodes generated up until the time limit was used to calculate the average and marked with an asterisk (*).
- # CG_{opt}: the average number of problems that the root node CG provided integer solutions.
- Gap_{int}: the average of the integrality gap between the optimal solution and the LP bound of the EF provided by the CG algorithm. For the problems by which we do not have optimal solutions, the best feasible solutions found from any algorithm are used and marked with an asterisk (*). If the root node CG is not finished, the lower bound of the RMLP is used as the LP relaxation bound, and the problem class is marked with a dagger symbol (†). $Gap_{int} = \frac{\text{(Optimal solution)}}{\text{(LP bound of the EF)}} \times 100\%$
- # Gap_{int}: the number of problems that have values of Gap_{int} less than a certain criteria. That is, the value of the Gap_{int} should be less than 100.5% or 105% to be counted in the columns "$< 0.5\%$" or "$< 5\%$," respectively.

TABLE VI
RESULTS RELATED TO THE CG AND B&P ALGORITHM

Problem Class	Cols		Nodes
	CG	B&P	B&P
C11	75.9	131.8	5.9
C13	173.6	271.2	14.0
C23	252.1	1,089.5*	351.8*
C210	1,682.5	2,214.2*	14.0*
C320	4,902.1*	4,902.1*	-*

$*$: There are instances not solved within the time limit.
$-$: There is no instance with the finished root node CG.

TABLE VII
RESULTS RELATED TO THE EF AND THE CG ALGORITHM

Problem Class	# CG_{opt}	Gap_{int} (%)	# Gap_{int}	
			$< 0.5\%$	$< 5\%$
C11	7	104.7	8	8
C13	6	101.5	7	9
C23	0	104.4	1	7
C210	0	103.8*	0*	8*
C320	-	122.2*†	0*†	0*†

$*$: There are instances that used the BFS to calculate the integrality gap.
† : Lower bound of the RMLP is used to calculate the integrality gap.

In Table VI, it is shown that as the size of the problem increased, the number of columns and nodes required followed. Note that the optimization process of the large-sized problems was not fully terminated, and the additional columns and nodes would be generated afterwards. In the RSF model, C210 and C320 consisted of 4,060 and 12,090 variables,

TABLE VIII
RESULTS OF THE RMH RELATED TO THE COMPUTATION SPEED

Problem Class	$\#\ solved$			$Time\ (s)$			$GapL\ (\%)$		
	RT	1200	2400	RT	1200	2400	RT	1200	2400
C11	10	10	10	0.08	0.44	0.44	0.0	0.0	0.0
C13	10	10	10	0.79	8.52	8.52	0.0	0.0	0.0
C23	10	10	10	0.86	370.29	735.22	0.0	0.0	0.0
C210	7	8	7	2,169.55*	2,319.65*	2,998.55*	1.2	0.9	2.2
C320	-	0	0	-	3,600*	3,600*		19.2	27.1†

$*$: There are instances not solved within the time limit.
† : There is an instance that a feasible solution is not found within the time limit.

respectively. Compared to the variables generated in B&P algorithms, the RSF models tended to be larger in sizes.

In Table VII, the performance of both the EF and the CG algorithm was analyzed from the integrality gap point-of-view. In the small-sized problems, the CG algorithm provided an integer optimal solution for 13 out of 30 instances, which did not require the additional branching process. The smaller integrality gap indicates the advantage of the EF. In the problem classes C11 and C13, 15 out of 20 instances had an integrality gap of less than 0.5%. In the larger problems, the integrality gap increased. However, it should be considered that in these problems, the BFS was used instead of the optimal solution because the large-sized problems were not solved to the optimal. Besides, for the class C320, the LP bound would also be improved when the CG is solved to the optimal.

The performances of the restricted master heuristics were tested in the third analysis. The RMH was proposed to solve the large-sized problem in a real-world situation in a time-efficient manner. As mentioned in Section IV-G, the RMH could be initiated at any stage of the B&P algorithm. The feasibility of the RMH was secured based on the initial columns, which were generated according to every possible pairing of a demand point and a facility. We compared three initiation points of the RMH. The first point was the well-known price-and-branch, where the RMH started after the root node CG is terminated. The second and third points were defined based on the computation time. Because the computation time limit is set to 3,600 seconds, we tested to start the RMH 1,200 and 2,400 seconds after the beginning of the B&P algorithm. Three initiation points are named in Tables VIII and IX as "RT," "1200," and "2400," respectively. In Table IX, column "# $(same, better)\ BFS$" represents the number of problems that the RMH algorithm provided the same or better BFS than the RSF.

In the RMH with the second and third starting points, there were problems solved by the B&P before the RMH was initiated. Every instance in problem classes C11 and C13, and eight instances in problem class C23 were solved before the RMH was started at 1200. Even for the RMH, problem class C320 was hard to solve within the time limitation of 3,600 seconds, however. Nevertheless, the RMH had relatively smaller $GapL$ than did the RSF, where the CG provided a better LP bound, and the heuristic provided a decent feasible solution.

TABLE IX
RESULTS OF THE RMH RELATED TO THE OPTIMALITY

Problem Class	$Gap\ (\%)$			$\#\ (same, better)\ BFS$		
	RT	1200	2400	RT	1200	2400
C11	0.9	0.0	0.0	(7, 0)	(10, 0)	(10, 0)
C13	0.3	0.0	0.0	(8, 0)	(10, 0)	(10, 0)
C23	1.6	0.0	0.0	(2, 0)	(10, 0)	(10, 0)
C210	4.2	4.5	3.2	(0, 0)	(0, 0)	(0, 1)
C320	-	8.5	14.9†	-	(0, 4)	(0, 3)

† : There is an instance that a feasible solution is not found within the time limit.

Table IX compared the optimality of the RMH to the RSF. In the RMH with the starting point of 1,200 seconds (RMH_1200), the optimal solution was found for every instance of the small-sized dataset. For the large-sized problem class, C210 and C320 had 4.5 and 8.5 percent of an average optimality gap, respectively. Furthermore, in problem class C320, RMH_1200 provided better BFS than RSF in four instances. The effective starting point of the RMH would be affected by each problem situation, and a further investigation is required when implemented in the applications.

To summarize, even though the built-in root cutting and heuristic algorithms in the commercial solver could provide a stronger feasible solution for the RSF than could the proposed algorithm, the fundamental intractability of the problem hinders the RSF from being solved because of the bad lower bound. However, the EF provided a strong LP relaxation bound and had a competent integrality gap, and the B&P algorithm was expected to show a good performance in the lower bound point of view. The RMH could be implemented in the B&P algorithm to find primal bounds used in the branching. In the large-scale problems, it was observed that the RMH could provide time-efficient solutions. Because the RMH optimizes the batch decisions developed through the CG process, the heuristic can avoid the long convergence time that the RSF faces.

VI. CONCLUSION

This paper introduced the location and allocation problem of UAVs in the emergency medical service system considering demand uncertainties. A UAV-operated system would

seemingly lead to new operation problems, which would make applying the solution approach from existing literature difficult. The UEMS system, instead of using one or two UAVs, could use a fleet of UAVs operating from a facility. Furthermore, the number of UAVs employed plays an essential role in defining the capability of a facility. The resource availability is modeled to increase gradually along with the number of UAVs, which is considered when allocating demand points to a facility. In the ULAP, both the variable coverage distance and the capacity of the UEMS facility are modeled as functions of the number of UAVs. First, the quadratic constraint of the variable coverage distance is linearized. Second, the demand is modeled based on the cardinality-constrained uncertainty set, and the resultant nonlinear capacity constraint of the model is reformulated to the MILP model.

However, because of the highly fractional solution of the LP relaxation, the reformulated standard formulation of the ULAP has a weak LP relaxation bound and is challenging to solve with a commercial solver. An extended formulation and a B&P algorithm was proposed in this paper to improve the LP bound and utilize it. Because of the Ryan-Foster branching strategy and the corresponding disjunctive constraints, the subproblem is defined as a robust disjunctively constrained integer knapsack problem. Based on the existing knowledge about various types of knapsack problems, a decomposed DP approach was proposed as a special-purpose solver. A hybrid approach of the MILP and the decomposed DP approach was also introduced. A restricted master heuristic was proposed for a primal solution based on the EF.

In the computational experiment comparing the performance of the RSF and the EF and the corresponding B&P algorithm, the EF showed stronger LP bounds. Despite the weak LP bound, in small-sized problems, the RSF could find the optimal solution in a short computation time by virtue of root cutting and heuristics. In larger problems, the RSF reported a large Gap_L, which represented a slow convergence of the algorithm. Even though the EF showed the better bound, the B&P algorithm could not provide feasible solutions for large-sized problems because the algorithm depended on the best-first search. The restricted master heuristic is developed to utilize the columns found through the CG process and could provide time-efficient feasible solutions. In the largest problem class, C320, the RMH could find even better feasible solutions than the RSF.

In this research, the RMH was initiated after the discontinuation of the B&P algorithm to measure the sole performance of the RMH. However, it is expected that the RMH could provide the primal bounds if implemented in the middle of the B&P algorithm, and could thereby help the searching process. Also, because the heuristics in the commercial solver provided effective feasible solutions for RSF, they could be used for the initial columns. For future research, more realistic problems could be solved with actual datasets. For an actual cost-benefit analysis, complex cases could be modeled with triage [77], patient behaviors [78], and multiple levels of hospitals [77]. More advanced busy-fraction models can be used while defining the variable coverage distance. In this research, commercial solver was used to solve the subproblem with the MILP reformulation approach without using the structural knowledge. However, one can refer to Ben Salem et al. [79], who studied the polytope and the facet defining inequalities of the disjunctive-constrained knapsack problem. Atamtürk studied the inequalities on covers and packs of the integer knapsack sets [80] and focused on the convex hull of the robust knapsack problem [60]. Another research extension related to the health care facility location problem is the data-driven and dynamic relocation of UAVs among the UEMS facilities.

ACKNOWLEDGMENT

The authors would like to thank the Editor-in-Chief, the Editor, and the anonymous reviewers for their constructive comments and suggestions to improve this manuscript.

REFERENCES

[1] M. P. Larsen, M. S. Eisenberg, R. O. Cummins, and A. P. Hallstrom, "Predicting survival from out-of-hospital cardiac arrest: A graphic model," *Ann. Emergency Med.*, vol. 22, no. 11, pp. 1652–1658, Nov. 1993.

[2] L. Zhen, K. Wang, and H. C. Liu, "Disaster relief facility network design in metropolises," *IEEE Trans. Syst., Man, Cybern., Syst.*, vol. 45, no. 5, pp. 751–761, May 2015.

[3] A. V. Savkin and H. Huang, "Range-based reactive deployment of autonomous drones for optimal coverage in disaster areas," *IEEE Trans. Syst. Man, Cybern. Syst.*, vol. 51, no. 7, pp. 4606–4610, Jul. 2021.

[4] C. Wankmüller, C. Truden, C. Korzen, P. Hungerländer, E. Kolesnik, and G. Reiner, "Optimal allocation of defibrillator drones in mountainous regions," *OR Spectr.*, vol. 42, no. 3, pp. 785–814, Sep. 2020.

[5] S. Sawadsitang, D. Niyato, P.-S. Tan, and P. Wang, "Joint ground and aerial package delivery services: A stochastic optimization approach," *IEEE Trans. Intell. Transp. Syst.*, vol. 20, no. 6, pp. 2241–2254, Jun. 2019.

[6] H. Y. Jeong, B. D. Song, and S. Lee, "The flying warehouse delivery system: A quantitative approach for the optimal operation policy of airborne fulfillment center," *IEEE Trans. Intell. Transp. Syst.*, vol. 22, no. 12, pp. 7521–7530, Dec. 2021.

[7] D. N. Das, R. Sewani, J. Wang, and M. K. Tiwari, "Synchronized truck and drone routing in package delivery logistics," *IEEE Trans. Intell. Transp. Syst.*, vol. 22, no. 9, pp. 5772–5782, Sep. 2021.

[8] B. Purahong, T. Anuwongpinit, A. Juhong, I. Kanjanasurat, and C. Pintaviooj, "Medical drone managing system for automated external defibrillator delivery service," *Drones*, vol. 6, no. 4, p. 93, Apr. 2022.

[9] J. K. Zègre-Hemsey, B. Bogle, C. J. Cunningham, K. Snyder, and W. Rosamond, "Delivery of automated external defibrillators (AED) by drones: Implications for emergency cardiac care," *Current Cardiovascular Risk Rep.*, vol. 12, no. 11, pp. 1–5, Nov. 2018.

[10] G. Ling and N. Draghic, "Aerial drones for blood delivery," *Transfusion*, vol. 59, no. S2, pp. 1608–1611, Apr. 2019.

[11] C. A. Thiels, J. M. Aho, S. P. Zietlow, and D. H. Jenkins, "Use of unmanned aerial vehicles for medical product transport," *Air Med. J.*, vol. 34, no. 2, pp. 104–108, 2015.

[12] L. A. Haidari et al., "The economic and operational value of using drones to transport vaccines," *Vaccine*, vol. 34, pp. 4062–4067, Jul. 2016.

[13] K. Sharma, H. Singh, D. K. Sharma, A. Kumar, A. Nayyar, and R. Krishnamurthi, "Dynamic models and control techniques for drone delivery of medications and other healthcare items in COVID-19 hotspots," in *Emerging Technologies for Battling COVID-19. Studies in Systems, Decision and Control*, vol. 324, F. Al-Turjman, A. Devi, and A. Nayyar, Eds. Cham, Switzerland: Springer, 2021, pp. 1–34.

[14] A. Y. Chen and T.-Y. Yu, "Network based temporary facility location for the emergency medical services considering the disaster induced demand and the transportation infrastructure in disaster response," *Transp. Res. B, Methodol.*, vol. 91, pp. 408–423, Sep. 2016.

[15] Y. Liu, N. Cui, and J. Zhang, "Integrated temporary facility location and casualty allocation planning for post-disaster humanitarian medical service," *Transp. Res. E, Logistics Transp. Rev.*, vol. 128, pp. 1–16, Aug. 2019.

[16] W. Wang, K. Yang, L. Yang, and Z. Gao, "Two-stage distributionally robust programming based on worst-case mean-CVaR criterion and application to disaster relief management," *Transp. Res. E, Logistics Transp. Rev.*, vol. 149, May 2021, Art. no. 102332.

[17] C.-C. Chou, W.-C. Chiang, and A. Y. Chen, "Emergency medical response in mass casualty incidents considering the traffic congestions in proximity on-site and hospital delays," *Transp. Res. E, Logistics Transp. Rev.*, vol. 158, Feb. 2022, Art. no. 102591.

[18] Y. Zhou, J. Liu, Y. Zhang, and X. Gan, "A multi-objective evolutionary algorithm for multi-period dynamic emergency resource scheduling problems," *Transp. Res. E, Logistics Transp. Rev.*, vol. 99, pp. 77–95, Mar. 2017.

[19] T. Kundu, J.-B. Sheu, and H.-T. Kuo, "Emergency logistics management—Review and propositions for future research," *Transp. Res. E, Logistics Transp. Rev.*, vol. 164, Aug. 2022, Art. no. 102789.

[20] A. P. Iannoni and R. Morabito, "A multiple dispatch and partial backup hypercube queuing model to analyze emergency medical systems on highways," *Transp. Res. E, Logistics Transp. Rev.*, vol. 43, no. 6, pp. 755–771, Nov. 2007.

[21] S. Ansari, S. Yoon, and L. A. Albert, "An approximate hypercube model for public service systems with co-located servers and multiple response," *Transp. Res. E, Logistics Transp. Rev.*, vol. 103, pp. 143–157, Jul. 2017.

[22] S. Yoon and L. A. Albert, "A dynamic ambulance routing model with multiple response," *Transp. Res. E, Logistics Transp. Rev.*, vol. 133, Jan. 2020, Art. no. 101807.

[23] S. Yoon and L. A. Albert, "Dynamic dispatch policies for emergency response with multiple types of vehicles," *Transp. Res. E, Logistics Transp. Rev.*, vol. 152, Aug. 2021, Art. no. 102405.

[24] Z. Zhang, H. Qin, K. Wang, H. He, and T. Liu, "Manpower allocation and vehicle routing problem in non-emergency ambulance transfer service," *Transp. Res. E, Logist. Transp. Rev.*, vol. 106, pp. 45–59, Oct. 2017.

[25] H. Park, A. Shafahi, and A. Haghani, "A stochastic emergency response location model considering secondary incidents on freeways," *IEEE Trans. Intell. Transp. Syst.*, vol. 17, no. 9, pp. 2528–2540, Sep. 2016.

[26] Y.-C. Lee, Y.-S. Chen, and A. Y. Chen, "Lagrangian dual decomposition for the ambulance relocation and routing considering stochastic demand with the truncated Poisson," *Transp. Res. B, Methodol.*, vol. 157, pp. 1–23, Mar. 2022.

[27] M. S. Daskin, "What you should know about location modeling," *Nav. Res. Logistics*, vol. 55, no. 4, pp. 283–294, 2008.

[28] Z. Drezner, K. Klamroth, A. Schöbel, and G. O. Wesolowsky, "The Weber problem," in *Facility Location: Applications and Theory*, Z. Drezner and H. W. Hamacher, Eds. Cham, Switzerland: Springer, 2001, pp. 1–36.

[29] F. Plastria, "Continuous covering location problems," in *Facility Location: Applications and Theory*, Z. Drezner and H. W. Hamacher, Eds. Springer, 2001, pp. 37–79, doi: 10.1007/978-3-642-56082-8_2.

[30] M. S. Daskin and K. L. Maass, "The p-median problem," in *Location Science*, G. Laporte, S. Nickel, and F. S. da Gama, Eds. Cham, Switzerland: Springer, 2015, pp. 21–45.

[31] H. Calik, M. Labbé, and H. Yaman, "P-center problems," in *Location Science*, G. Laporte, S. Nickel, and F. S. da Gama, Eds. Cham, Switzerland: Springer, 2015, pp. 79–92.

[32] C. Toregas, R. Swain, C. ReVelle, and L. Bergman, "The location of emergency service facilities," *Oper. Res.*, vol. 19, no. 6, pp. 1363–1373, 1971.

[33] I.-C. Choi and S. S. Chaudhry, "The p-median problem with maximum distance constraints: A direct approach," *Locat. Sci.*, vol. 1, no. 3, pp. 235–243, 1993.

[34] G. Avellar, G. Pereira, L. Pimenta, and P. Iscold, "Multi-UAV routing for area coverage and remote sensing with minimum time," *Sensors*, vol. 15, no. 11, pp. 27783–27803, Nov. 2015.

[35] S. Kim and I. Moon, "Traveling salesman problem with a drone station," *IEEE Trans. Syst., Man, Cybern. Syst.*, vol. 49, no. 1, pp. 42–52, May 2019.

[36] A. Ghaddar, A. Merei, and E. Natalizio, "PPS: Energy-aware grid-based coverage path planning for UAVs using area partitioning in the presence of NFZs," *Sensors*, vol. 20, no. 13, p. 3742, Jul. 2020.

[37] Y. Liu, Z. Liu, J. Shi, G. Wu, and W. Pedrycz, "Two-echelon routing problem for parcel delivery by cooperated truck and drone," *IEEE Trans. Syst. Man, Cybern. Syst.*, vol. 51, no. 12, pp. 7450–7465, Dec. 2021.

[38] M. S. Daskin, "A maximum expected covering location model: Formulation, properties and heuristic solution," *Transp. Sci.*, vol. 17, no. 1, pp. 48–70, Feb. 1983.

[39] C. ReVelle and K. Hogan, "The maximum availability location problem," *Transp. Sci.*, vol. 23, no. 3, pp. 192–200, Aug. 1989.

[40] H. Shakhatreh, A. Khreishah, J. Chakareski, H. B. Salameh, and I. Khalil, "On the continuous coverage problem for a swarm of UAVs," in *Proc. IEEE 37th Sarnoff Symp.*, Sep. 2016, pp. 130–135.

[41] C. Wang, Z. Wang, Y. Tian, X. Zhang, and J. Xiao, "A dual-population based evolutionary algorithm for multi-objective location problem under uncertainty of facilities," *IEEE Trans. Intell. Transp. Syst.*, vol. 23, no. 7, pp. 7692–7707, Jul. 2022.

[42] M. Gendreau, G. Laporte, and F. Semet, "Solving an ambulance location model by Tabu search," *Location Sci.*, vol. 5, no. 2, pp. 75–88, Aug. 1997.

[43] Z.-H. Zhang and H. Jiang, "A robust counterpart approach to the bi-objective emergency medical service design problem," *Appl. Math. Model.*, vol. 38, no. 3, pp. 1033–1040, Feb. 2014.

[44] P. Beraldi and M. E. Bruni, "A probabilistic model applied to emergency service vehicle location," *Eur. J. Oper. Res.*, vol. 196, no. 1, pp. 323–331, Jul. 2009.

[45] D. Bertsimas and Y. Ng, "Robust and stochastic formulations for ambulance deployment and dispatch," *Eur. J. Oper. Res.*, vol. 279, no. 2, pp. 557–571, Dec. 2019.

[46] O. Berman, D. Krass, and Z. Drezner, "The gradual covering decay location problem on a network," *Eur. J. Oper. Res.*, vol. 151, no. 3, pp. 474–480, Dec. 2003.

[47] H. A. Eiselt and V. Marianov, "Gradual location set covering with service quality," *Socio-Econ. Planning Sci.*, vol. 43, no. 2, pp. 121–130, Jun. 2009.

[48] H. Jang and T. Lee, "Demand point aggregation method for covering problems with gradual coverage," *Comput. Oper. Res.*, vol. 60, pp. 1–13, Aug. 2015.

[49] O. Berman, Z. Drezner, D. Krass, and G. O. Wesolowsky, "The variable radius covering problem," *Eur. J. Oper. Res.*, vol. 196, no. 2, pp. 516–525, Jul. 2009.

[50] S. Akl, R. Benkoczi, D. R. Gaur, H. Hassanein, S. Hossain, and M. Thom, "On a class of covering problems with variable capacities in wireless networks," *Theor. Comput. Sci.*, vol. 575, pp. 42–55, Apr. 2015.

[51] O. Berman, Z. Drezner, and D. Krass, "Generalized coverage: New developments in covering location models," *Comput. Oper. Res.*, vol. 37, no. 10, pp. 1675–1687, Oct. 2010.

[52] V. Bélanger, A. Ruiz, and P. Soriano, "Recent optimization models and trends in location, relocation, and dispatching of emergency medical vehicles," *Eur. J. Oper. Res.*, vol. 272, no. 1, pp. 1–23, 2019.

[53] A. Ahmadi-Javid, P. Seyedi, and S. S. Syam, "A survey of healthcare facility location," *Comput. Oper. Res.*, vol. 79, pp. 223–263, Mar. 2017.

[54] Z.-H. Zhang and K. Li, "A novel probabilistic formulation for locating and sizing emergency medical service stations," *Ann. Oper. Res.*, vol. 229, no. 1, pp. 813–835, Jun. 2015.

[55] D. Bertsimas and M. Sim, "The price of robustness," *Oper. Res.*, vol. 52, no. 1, pp. 35–53, Jan. 2004.

[56] A. L. Soyster, "Technical note—Convex programming with set-inclusive constraints and applications to inexact linear programming," *Oper. Res.*, vol. 21, no. 5, pp. 1154–1157, Oct. 1973.

[57] A. Ben-Tal and A. Nemirovski, "Robust solutions of linear programming problems contaminated with uncertain data," *Math. Program.*, vol. 88, no. 3, pp. 411–424, 2000.

[58] R. C. Larson, "A hypercube queuing model for facility location and redistricting in urban emergency services," *Comput. Oper. Res.*, vol. 1, no. 1, pp. 67–95, Mar. 1974.

[59] P. L. van den Berg, G. J. Kommer, and B. Zuzáková, "Linear formulation for the maximum expected coverage location model with fractional coverage," *Oper. Res. Health Care*, vol. 8, pp. 33–41, Mar. 2016.

[60] A. Atamtürk, "Strong formulations of robust mixed 0–1 programming," *Math. Program.*, vol. 108, nos. 2–3, pp. 235–250, Sep. 2006.

[61] Y. Pochet and L. A. Wolsey, "Integer knapsack and flow covers with divisible coefficients: Polyhedra, optimization and separation," *Discrete Appl. Math.*, vol. 59, no. 1, pp. 57–74, Apr. 1995.

[62] S. Ceria, C. Cordier, H. Marchand, and L. A. Wolsey, "Cutting planes for integer programs with general integer variables," *Math. Program.*, vol. 81, no. 2, pp. 201–214, Apr. 1998.

[63] C. Barnhart, E. L. Johnson, G. L. Nemhauser, M. W. P. Savelsbergh, and P. H. Vance, "Branch-and-price: Column generation for solving huge integer programs," *Oper. Res.*, vol. 46, no. 3, pp. 316–329, 1998.

[64] D. M. Ryan and B. A. Foster, "An integer programming approach to scheduling," in *Computer Scheduling of Public Transport*, A. Wren, Ed. Elsevier, 1981, pp. 269–280.

[65] R. Sadykov and F. Vanderbeck, "Bin packing with conflicts: A generic branch-and-price algorithm," *INFORMS J. Comput.*, vol. 25, no. 2, pp. 244–255, May 2013.
[66] T. Yamada, S. Kataoka, and K. Watanabe, "Heuristic and exact algorithms for the disjunctively constrained knapsack problem," *Inf. Process. Soc. Jpn. J.*, vol. 43, no. 9, pp. 1–7, 2002.
[67] S. Elhedhli, L. Li, M. Gzara, and J. Naoum-Sawaya, "A Branch-and-Price algorithm for the bin packing problem with conflicts," *INFORMS J. Comput.*, vol. 23, no. 3, pp. 404–415, Aug. 2011.
[68] F. Vanderbeck, "Branching in branch-and-price: A generic scheme," *Math. Program.*, vol. 130, no. 2, pp. 249–294, Dec. 2011.
[69] D. Bertsimas and M. Sim, "Robust discrete optimization and network flows," *Math. Program.*, vol. 98, nos. 1–3, pp. 49–71, 2003.
[70] C. Lee, K. Lee, K. Park, and S. Park, "Technical note—Branch-and-price-and-cut approach to the robust network design problem without flow bifurcations," *Oper. Res.*, vol. 60, no. 3, pp. 604–610, Jun. 2012.
[71] U. Pferschy and J. Schauer, "The knapsack problem with conflict graphs," *J. Graph Algorithms Appl.*, vol. 13, no. 2, pp. 233–249, 2009.
[72] R. Sadykov, F. Vanderbeck, A. Pessoa, I. Tahiri, and E. Uchoa, "Primal heuristics for branch and price: The assets of diving methods," *INFORMS J. Comput.*, vol. 31, no. 2, pp. 251–267, Apr. 2019.
[73] E. Alekseeva, N. Kochetova, Y. Kochetov, and A. Plyasunov. *Benchmark library Discrete Location Problems*. Accessed: Nov. 19, 2022. [Online]. Available: http://old.math.nsc.ru/AP/benchmarks/english.html
[74] S. M. Shavarani, M. G. Nejad, F. Rismanchian, and G. Izbirak, "Application of hierarchical facility location problem for optimization of a drone delivery system: A case study of Amazon prime air in the city of San Francisco," *Int. J. Adv. Manuf. Technol.*, vol. 95, nos. 9–12, pp. 3141–3153, Apr. 2018.
[75] Y. Park, S. Lee, I. Sung, P. Nielsen, and I. Moon. *Benchmark Facility Location-Allocation Problem for Emergency Medical Service with Unmanned Aerial Vehicle*. Accessed: Nov. 19, 2022. [Online]. Available: http://scm.snu.ac.kr/research/ULAP_DATA.zip
[76] F. Vanderbeck and L. A. Wolsey, "Reformulation and decomposition of integer programs," in *50 Years Integer Program. 1958–2008*. Cham, Switzerland: Springer, 2010, pp. 431–502.
[77] K. Shin and T. Lee, "Emergency medical service resource allocation in a mass casualty incident by integrating patient prioritization and hospital selection problems," *IISE Trans.*, vol. 52, no. 10, pp. 1141–1155, Oct. 2020.
[78] H. Jang, K. Hwang, T. Lee, and T. Lee, "Designing robust rollout plan for better rural perinatal care system in Korea," *Eur. J. Oper. Res.*, vol. 274, no. 2, pp. 730–742, Apr. 2019.
[79] M. B. Salem, R. Taktak, A. R. Mahjoub, and H. Ben-Abdallah, "Optimization algorithms for the disjunctively constrained knapsack problem," *Soft Comput.*, vol. 22, no. 6, pp. 2025–2043, Mar. 2018.
[80] A. Atamtürk, "Cover and pack inequalities for (mixed) integer programming," *Ann. Oper. Res.*, vol. 139, no. 1, pp. 21–38, Oct. 2005.

Youngsoo Park received the Ph.D. degree in industrial engineering from Seoul National University in 2021. He is currently a Data Scientist at Woowa Brothers Corporation. His major research interests include modeling and optimization of operation problems in transportation systems and logistics.

Sangyoon Lee received the Ph.D. degree in industrial engineering from Seoul National University in 2020. He is currently a Staff Researcher at the Samsung Advanced Institute of Technology. His research interests are in the area of system design and scheduling of automated systems, especially for lab automation.

Inkyung Sung received the Ph.D. degree in industrial engineering from the Korea Advanced Institute of Science and Technology in 2016. He is currently an Assistant Professor at the Operations Research Group, Department of Materials and Production, Aalborg University, Denmark. His research interests are in the area of system design and modeling, primarily applying operations research techniques.

Peter Nielsen received the M.Sc. and Ph.D. degrees in engineering from Aalborg University, Denmark, in 2005 and 2008, respectively. He is currently an Associate Professor at the Department of Materials and Production, Aalborg University. He has been heading the Operations Research Group since 2011. He was the Chief Editor for the journal *Production and Manufacturing Research* for nine years (2013–2021). His research areas lie within artificial intelligence for autonomous (cyber-physical) systems, with a special emphasis on NP-hard problems that need to be solved in real-time or near real-time. He has a particular interest in unmanned systems and their applications. He has coauthored more than 50 journals and numerous contributions to conferences papers and books.

Ilkyeong Moon received the B.S. and M.S. degrees in industrial engineering from Seoul National University, South Korea, and the Ph.D. degree in operations research from Columbia University. He is currently a Professor in industrial engineering at Seoul National University. He has published over 130 articles in international journals. His research interests include supply chain management, logistics, and inventory management. He was the President of the Korean Institute of Industrial Engineers (KIIE) from 2019 to 2020. He is a fellow of the Asia–Pacific Industrial Engineering and Management Society. He is the Vice Chair of WG 5.7 of IFIP. He was the Former Editor-in-Chief of *Journal of the Korean Institute of Industrial Engineers*, which is a flagship journal of KIIE. He serves as an Associate Editor for several journals, including *European Journal of IE* and *Flexible Services and Manufacturing*.